ADVANCED PASSIVE SAFETY SYSTEMS FOR AIRCRAFT: NUMERICAL SIMULATION OF PARACHUTE INFLATION

Štěpán Kaspar[1] & Robert Grim[1]

[1]Faculty of Mechanical Engineering, Institute of Aerospace Engineering, Brno University of Technology, Brno, Czech Republic

Abstract

The rapid growth of urban air mobility necessitates the development of advanced passive safety systems for Vertical Take-Off and Landing (VTOL) aircraft. Traditional parachute recovery systems have proven effective for fixed-wing aircraft, but adapting them to VTOL's complex flight profile presents unique challenges. Existing systems work well during horizontal flight due to higher speeds and altitudes. However, the vertical and transitional flight phases require significantly faster parachute inflation to achieve effective deceleration within limited altitude, creating a trade-off between rapid inflation and potentially hazardous opening shocks that can subject passengers to dangerous G-forces.

This study explores using numerical simulations to accelerate parachute development for VTOL applications. Traditional methods, such as wind tunnel and drop testing, require the production of physical prototypes, which is both time-consuming and resource-intensive. This research proposes Fluid-Structure Interaction (FSI) analysis as a viable alternative. Previously the FSI analysis of the parachute was conducted using custom FSI solvers developed for example by Tezduyar [17] and others. LS-Dyna was used for parachute simulation employing the Arbitrary Lagrangian-Eulerian (ALE) approach by Tutt [19], which is more relevant to supersonic parachutes. Utilizing ANSYS LS-Dyna software with an Incompressible CFD (ICFD) solver is more suitable for subsonic parachutes. LeGarecc confirmed the possibility of using this solver [9]. Simulation in this study utilized ICFD solver and an implicit structural solver, which cooperated using two-way strong coupling to accurately model the dynamic interaction between the parachute and the surrounding air.

A detailed workflow for finite mass analysis was developed to predict parachute inflation with variable descent velocities, based on the generated drag forces. The canopy was modeled as a fabric material for airbag modeling, ensuring realistic deformation and performance characteristics. The suspension lines were treated as cables to represent their mechanical properties and behavior during deployment accurately. The parachute prototype used in this study is currently under development at the Institute of Aerospace Engineering at Brno University of Technology, and the simulation results showed sufficient correlation with existing experimental data.

Keywords: Parachute, Passive safety, FSI, numerical simulation, inflation

1. Introduction

1.1 Passive safety of an aircraft

Aviation is considered one of the safest ways of transport in the world, but the severity of air accidents is significantly higher than others. Due to higher certification requirements, the number of aviation accidents has been decreasing in recent years as evidenced by reports from aviation authorities [10, 11], but the proportion of fatal accidents remains the same. Ways to increase safety in critical situations include parachute rescue systems or the use of airbags.

Parachute rescue systems are now a compulsory part of small passenger aircraft in some countries. For example, in Germany parachute recovery system is mandatory for all ultralight aircraft based on DULV requirements. Even though recovery systems are not mandatory, aircraft manufactures are implementing these systems into the design based on customer's demands. These devices are capable of slowing a falling aircraft to a speed that is not fatal to humans. For a parachute rescue system to function properly, a number of conditions must be met, namely the minimum activation height required to inflate the parachute and slow the aircraft's fall. Minimum altitude and slow speed flight regimes are encountered especially by VTOL aircraft during vertical take-off, landing, and during hover.

VTOL aircraft have seen considerable development in recent years. Due to the nature of the flight mission, the aircraft can be flown or hovered at low altitudes, mainly in the vertical flight mode, as well as at higher altitudes. This brings new requirements for parachute rescue systems. The parachute has to meet fast inflation times for low altitudes, but at the same time acceptable shock loads for falls from higher altitudes. New parachutes or parachute inflation control systems meeting the above requirements while maintaining the minimum weight of the system are required.

1.2 Numerical modelling

The experimental methods used for the analysis of the aerodynamic properties of parachutes are: wind tunnel measurements and drop tests. These methods are representatives of infinite mass analysis and finite mass analysis. The first mentioned analysis gives us information about the generated overall drag and stability in steady-state free fall and the later mentioned gives us in addition information about the inflating shock, filling rate and time to reach steady descent.

Finite mass type analysis can be analysed using only CFD code using predicted inflated shape of an parachute constructed using CAD. This approach was tested multiple times but fails to provide accurate results because of big deflections of fabric and transient behavior [15, 1, 7, 14]. These methods cannot predict behavior during inflation.

Several approaches have been developed to model the interactions between fluid flow and flexible parachute structures using the Arbitrary Lagrangian-Eulerian (ALE) method and other advanced numerical techniques within commercial software like LS-Dyna. For instance, Tutt [20, 18] first introduced the ALE method for parachute behavior analysis, demonstrating reasonable correlation with experimental results, though without considering fabric porosity. Subsequent works by Coquet [21] and Tutt [19] improved this approach by incorporating the Ergun porosity model, enhancing the fidelity of steady-state simulations for cross parachutes. These models primarily focused on steady-state analyses, where simulations of inflated parachutes closely matched experimental observations [16, 19].

In recent years, the focus has shifted toward more sophisticated simulations, particularly for Ram-Air parachutes, where fluid dynamics play a critical role. Charles [4] utilized the Incompressible Computational Fluid Dynamics (ICFD) solver within LS-Dyna for FSI simulations of Ram-Air parachutes, providing a detailed examination of their aerodynamic behavior. Chambe [3] refined this by linking two-dimensional beam elements to three-dimensional shell elements, emphasizing the impact of ropes on drag. Perin [12] employed an ALE-based approach, achieving good shape correlation but highlighting discrepancies in aerodynamic properties. Legarecc [9] extended the ICFD solver application to spherical parachutes, using a Large Eddy Simulation (LES) turbulence model to analyze inflation from a spinetree configuration. These studies emphasize the complexities of FSI in parachute modeling, particularly in subsonic flows.

Various alternative methods have been explored in an effort to improve the accuracy of FSI simulations. Gao [6] developed a custom solver for simulating the inflation of a circular parachute under stochastic wind conditions, incorporating fabric permeability and achieving acceptable agreement with experimental data. Fagley [5] compared weakly coupled FSI simulations using separate solvers for the fluid and structural problems with fully coupled ALE simulations, demonstrating the advantages

of the latter approach in modeling complex interactions such as the behavior of bleed air spoilers on cruciform parachutes. Tezduyar [17] applied a space-time FSI solver to analyze the parachutes of the Orion space module, accounting for both subsonic and supersonic conditions. These works demonstrate a growing interest in refining the numerical modeling techniques to enhance the predictive capabilities of parachute simulations under various fluid-structure interaction scenarios.

In this research paper, the FSI simulation methodology for finite mass analysis of parachute inflation is presented. The simulation was performed using Ansys LS-Dyna, which provides the capability of a two-way strongly coupled FSI analysis employing an implicit structural solver and an ICFD flow solver. Comparisons of the inflation rate and the magnitude of the opening shock were made for different parachute activation descent rates.

2. Parachute geometry

The parachute that was analyzed was a spherical parachute with 8 chambers. The diameter of the parachute skirt in fully inflated form is $D_0 = 1,128\ m$. The resulting wetted area is $S_{wetted} = 1\ m^2$. The canopy is equipped with a vent hole with diameter $D_{vent} = 0.173\ m$. The suspension ropes had a length of $l_{suspension-line} = 1\ m$. The parachute was equipped with a riser to increase stability. The length of the riser was $l_{riser} = 0.75\ m$. This parachute is a development prototype for use in passive rescue systems for small transport aircraft.

3. Numerical model

An infinite mass type analysis was performed. The parachute was modeled in a spinetree configuration, which was released and allowed to analyze the inflation of the parachute.

3.1 Fluid model

The modelling of the flow field was based on the Incompressible CFD (ICFD) solver. The solver provides the possibility to model turbulent flow using traditional models: $k-\varepsilon$, $k-\omega$, LES. $k-\varepsilon$ was used as the turbulent model. The model was chosen mainly because of the absence of prismatic cells for boundary layer modelling. There is a significant separation of the flow at the parachute canopy throat, thus prismatic cells do not bring a more accurate calculation, on the contrary, their presence in the model significantly increased the risk of divergence.

The boundary conditions on the domain walls were ICFD-BOUNDARY-PRESCRIBED-PRE (outlet), ICFD-BOUNDARY-PRESCRIBED-VEL (inlet), ICFD-BOUNDARY-FREESLIP (surrounding walls), ICFD-BOUNDARY-NOSLIP (canopy). The outlet was prescribed atmospheric pressure for 0 m ISA (International standard atmosphere), and the inlet was prescribed constant velocity. These boundary conditions are equivalent to traditional boundary conditions in commercial CFD codes: pressure outlet, velocity inlet, and wall with and without shear stress.

First-order numerical schemes were used to increase the stability and convergence of the calculation. The time step was constant but varied depending on the free-stream velocities. To reduce computational time, the convergence criteria for the pressure and momentum equations have been reduced from the $10-8$ limit to $10-5$. The domain was cylindrical. The dimensions of the domain can be seen in Figure 1. The characteristic dimension considered was the diameter of the inflated canopy.

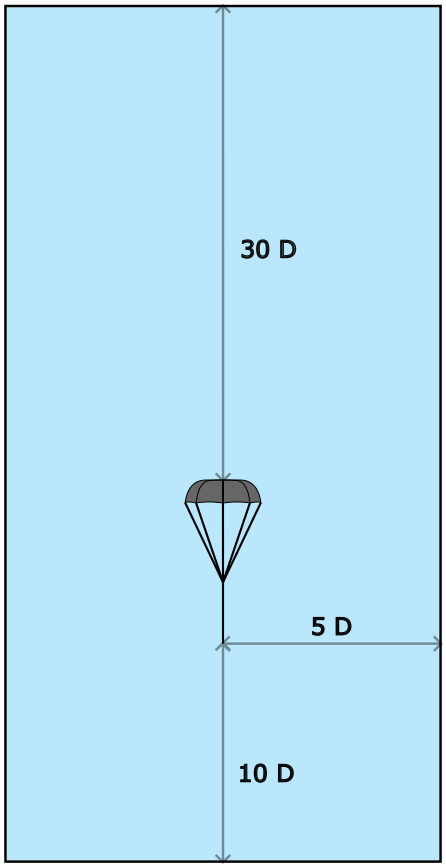

Figure 1 – Dimensions of fluid domain

The computational mesh consisted only of the surface mesh of the domain and canopy. Surface mesh can be seen in Figure 2 The surface mesh was triangular. The surface triangle mesh are the requirements of the ICFD solver since the volume meshing is solved automatically. Automatic remeshing was used, which is activated whenever the numerical error exceeds 5 percent or 200 iterations are reached. These settings were specified using ICFD ADAPT keyword with maintaining initial sizings. The suspension cables were not included in the flow field solution as they were modelled as member elements which cannot be projected into the volume mesh.

Since the canopy was modeled as a surface, it was necessary to project this surface into the computational domain. This was achieved using the MESH-EMBEDSHELL keyword. This keyword offsets this surface and creates 2 new ones. The spacing between these faces is a fairly critical parameter, as it must not be greater than the contact activation distance. If this rule is not followed the calculation divergence occurs. [13]

3.2 Structural model

The canopy fabric was modelled using shell elements. The numerical formulation of the elements was Fully-integrated shell element, which demonstrated better stability of the calculation compared to the Belytschko-Tsay formulation used in the [19] case. The material used was 034-Fabric, this material is used for modelling the canopy fabric. The material was originally designed to model airbags, which have similar properties to parachute fabric. The damping coefficient for the fabric was 0.05

The suspension lines were modeled as beam elements. The numerical formulation of the element was discrete beam/cable. This numerical formulation can be used with the 071-Cable discrete beam material. This combination was chosen because of the zero compressive stress, which is a characteristic behaviour of the ropes. The ropes are attached to each other and to the fabric by means of merging duplicated nodes. It is a rigid connection allowing rotation. The reinforcement of the material

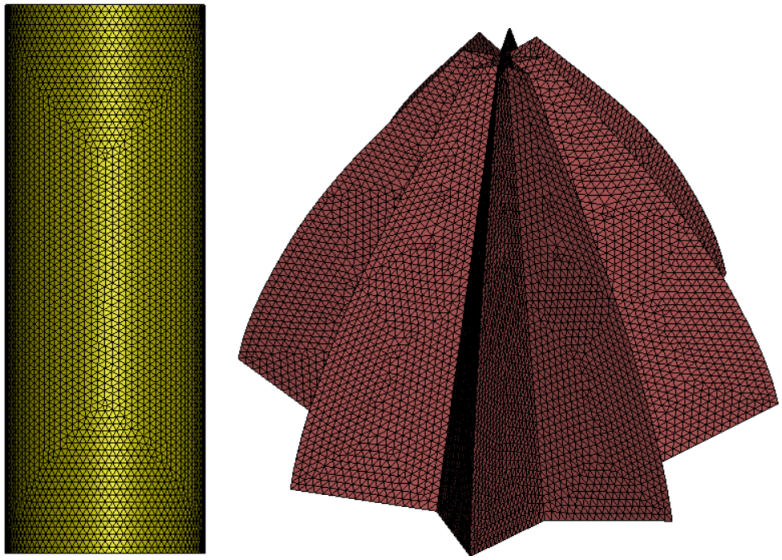

Figure 2 – CFD mesh

Property	Fabric	Supsension line
Young modulus	605 MPa	2.7 GPa
Density	656 $kg \cdot m^{-3}$	820 $kg \cdot m^{-3}$

Table 1 – Material properties

on the parachute can also be modelled in this way, but this was not used in the simulations.

Parachute was constrained in riser ending node was restricted from moving using BOUNDARY-SPC. Integration schemes for solving the dynamic behaviour of the parachute, namely the Newmark scheme and the Bath scheme, were compared. A comparison of these schemes was made by Borrwall [2] for rotating machines. The Bath scheme showed higher stability compared to the Newmark scheme. No difference on the results or stability of calculation was observed in the parachute inflation simulations. The newer Bath scheme was used. The solution was damped with the Bath integration scheme values $\gamma = 0.36$ and $\beta = 0.6$. The convergence criterion for the deformation was relative to the position of the nodes at the previous time step. The default setting compares the deformations to the initial state of the analysis. This method would cause convergence problems due to large deformations.

3.3 Fluid-Structure Interaction

FSI simulation is achieved by combining CSD and CFD solver. The solvers were fully coupled thus strong two-way FSI analysis was achieved. For this reason, it was necessary to use an implicit structural solver in conjunction with the ICFD solver. The number of sub-iterations of the FSI solver was limited to 200. Due to large deformations in lightweight structures (such as a parachute), oscillations can occur and significantly increase the computational time if sub-iterations are not limited. ICFD-BOUNDARY-FSI was used to specify the surfaces on which interaction between the CFD and CSD solver occurred. This boundary condition was applied to the parachute canopy, no-slip boundary condition still applies.

Interaction of the CSD and CFD solvers was initiated after reaching 0.05 s to avoid numerical errors by a fully undeveloped flow field.

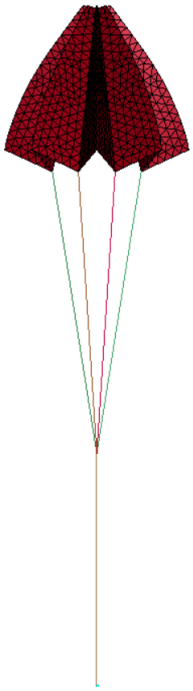

Figure 3 – FEM model of unfolded parachute

4. Results

Analyses of parachute inflation was conducted for range of different free-stream velocities from 2 m/s to 16 m/s. Drag forces were evaluated from reaction force in Z direction at place of boundary condition on riser. Reference area for calculation of drag coefficient was taken as wetted area of inflated canopy. No viscous drag was taken into account, only pressure forces. This was possible due to immediate separation of flow on the canopy edge. Drag coefficient for each analysis can be seen in Figure 4.
All simulations showcased the same behaviour at the beginning. Drag coefficient was small and than to zero dropped. This occurred around 0.05s. At that moment CFD and CSD interaction began. Canopy started to deform and move and thus drag force decreased. Canopy started to move and pressure gradient across canopy has not developed, thus the drop in drag coefficient. During the inflation of canopy snatch forces occurred. This behaviour is typical for parachute inflation. With higher free-stream velocities the time duration of peak load decreased.

Steady state phase after parachute inflation occurs in all cases after a time greater than $t = 0.5$ s. It can be observed that the drag coefficient oscillates around a constant value in all analyses. The oscillation is due to the numerical oscillation since the number of FSI sub-iterations was limited. The parachute did not exhibit unstable behavior at any free stream velocity, this would have resulted in a significant variation in the drag coefficient. However, it is possible that this behavior occurs later, as the parachutes were analyzed for 1 s. The drag coefficients for the steady-state phases of the parachutes can be seen in Figure 5. The drag coefficient does not change significantly with increasing ambient free-stream velocity. The slight decrease for higher velocities can be justified by the higher Reynolds number, which decreases the generated drag as it increases.

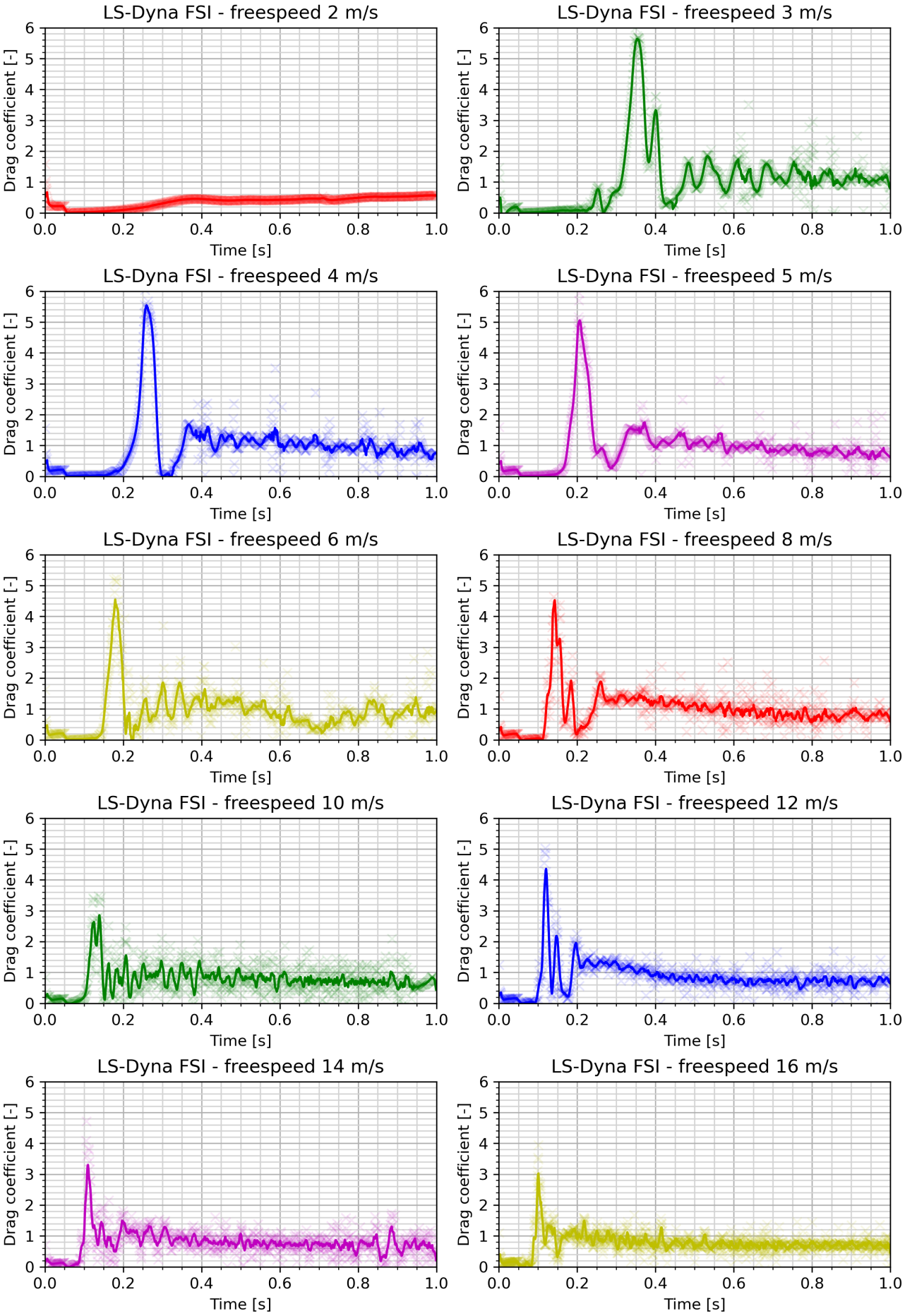

Figure 4 – Drag coefficient of inflation analyses

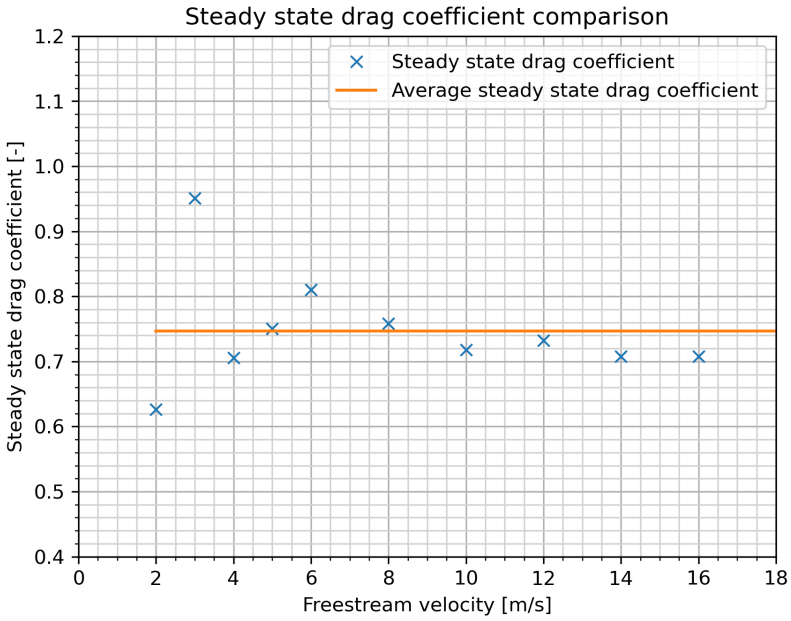

Figure 5 – Steady state drag coefficient comparison

In Figures 6 can be seen that with higher free-stream velocities the difference between snatch force coefficient and drag coefficient is decreasing this happens due to higher deformations of suspension lines. For low free-stream velocities the load in suspension lines is small and very small deformation occurs which increases the snatch force. With smaller air momentum the canopy is able to move in downwards direction and second force peak can be observed. This behaviour is non existent for free-stream velocities higher than $8\ m/s$. In Figure 6 can be seen very long filling time for free-stream velocity $2\ m/s$ and very small snatch coefficient. Inflation of the parachute into a fully inflated parachute does not occur, hence the time is long and a snatch shock is not observed. This behaviour can be expected, however, in real use this parachute is moving at this velocity in the steady-state deployment phase, where the inflation of the parachute has taken place at higher velocities.

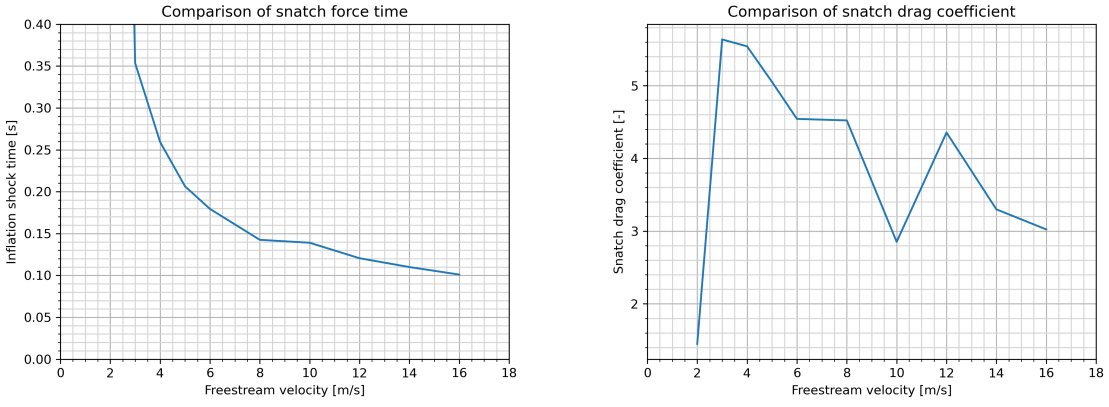

Figure 6 – Filling time

As mention in Knacke [8] inflation of a given parachute should open at fixed distance based on continuity law, in other words volume inside the canopy is the same regardless of free-stream velocities. This is described by specific filling distance (1), where n is parachute constant and D_o is parachute nominal diameter.

$$s_f = n \cdot D_o \tag{1}$$

$$t_f = \frac{n \cdot D_o}{v_\infty} \tag{2}$$

$$v_\infty \cdot t_f = n \cdot D_o \tag{3}$$

Filling time t_f is defined as (2). This equation can be rewritten as (3). Time to fill for infinite mass analysis is defined as time from moment of parachute release to point where maximum snatch force occurs. Product of free-stream velocity and filling time should be constant which is equal to specific filling distance. In Figure 7 can be seen specific filling distance for each free-stream velocity that was evaluated. Specific filling distance is almost equal for all free-stream velocities.

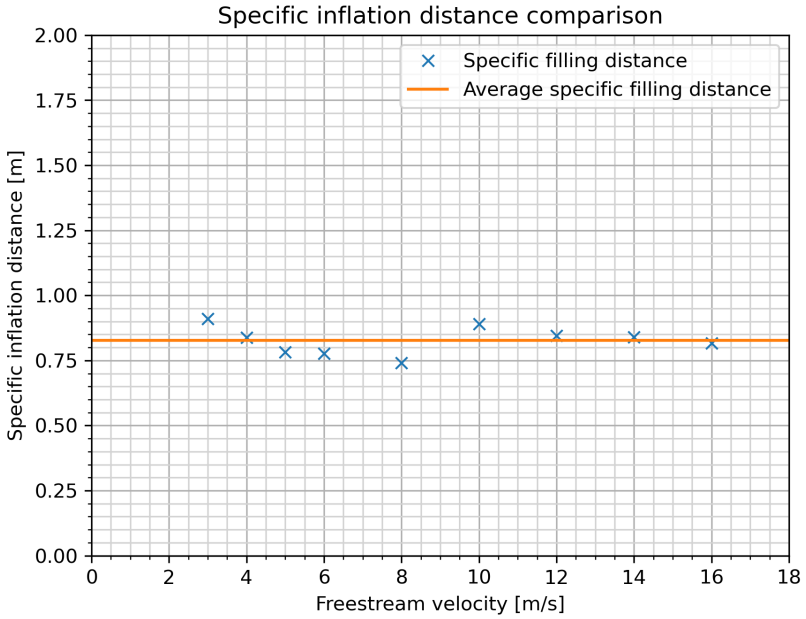

Figure 7 – Specific filling distance

4.1 Canopy deformation

In Figure 4 it can be seen that for free-stream velocities lower than 8 m/s the drag coefficient drops significantly after the moment of parachute filling, this is caused by the canopy moving upstream. At higher speeds this behaviour does not occur. This is due to the fact that the snatch force acting in the canopy at lower speeds overcomes the drag force. The energy stored in the deformations in the ropes is converted into kinetic energy of the canopy. However, at higher speeds, due to the higher momentum of the surrounding flow, this effect does not occur and the canopy does not change its inflated position. This behavior can be observed in Figure 8, which compares the shape of the canopy for $v_\infty = 3\ m/s$ and $v_\infty = 14\ m/s$.

From the moment the deformation and the position of the canopy reached steady state, the suspension lines started to oscillate. This phenomenon is caused by the absence of free-stream flow acting on the lines. The lines were modeled as 1-D Beam elements, which cannot be linked to a CFD solver. This oscillation represents an unrealistic phenomenon, but it did not affect the behavior of the parachute or the resulting generated drag forces. This behavior was less apparent with fewer elements forming a given line. For higher numbers of elements, significant numerical instabilities and divergence calculations occurred.

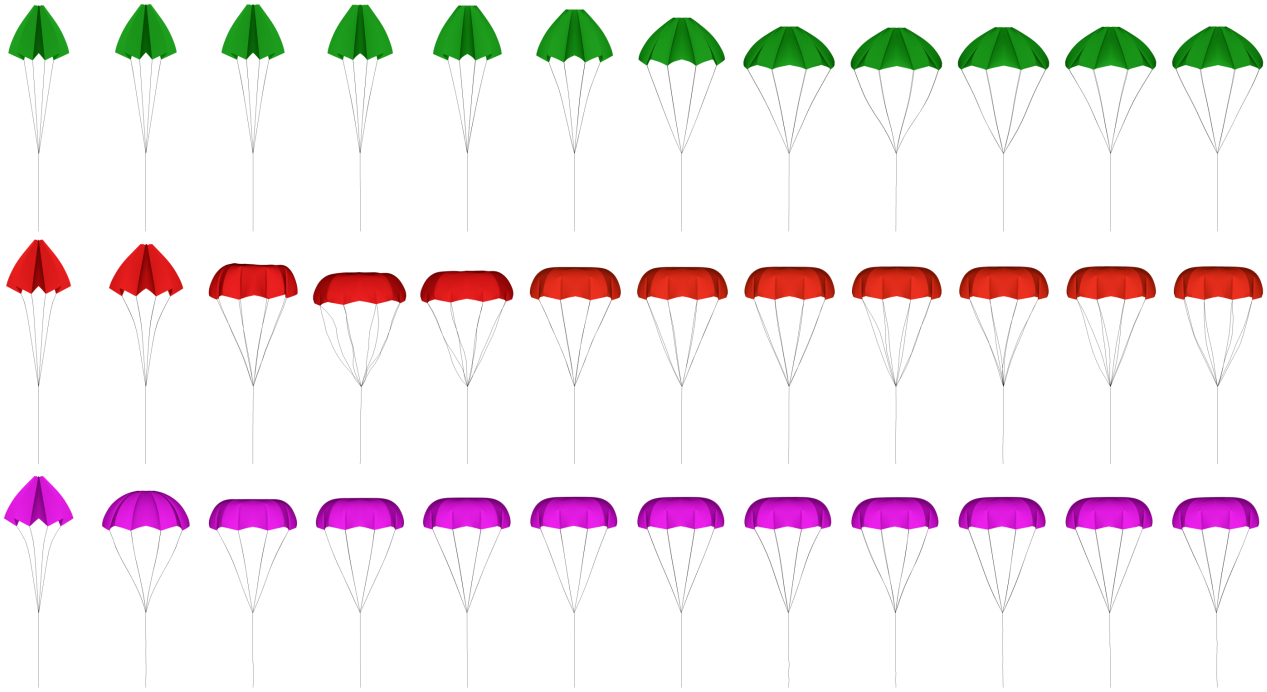

Figure 8 – Deformation of canopies for velocities: $3\ m/s$ (green),$8\ m/s$ (red), $14\ m/s$ (magenta). Time: 0.075s, 0.1s, 0.15s, 0.2s, 0.25s, 0.3s, 0,35s, 0.4s, 0.5s, 0.55s, 0.6s

In Figure 9 we can see the von Misses stresses in the fabric for steady state. The places of higher stress are in place of segment borders and in connection to the suspension lines. For higher free-stream velocities maximum stress is located in the edge of ventilation vent. The maximum stress values are at the point where the suspension lines are attached to the fabric. The fabric stresses do not exceed $\sigma_{VonMisses} = 120\ MPa$ for the highest free-stream velocity analysed and hence no fabric failure is expected during the drops.

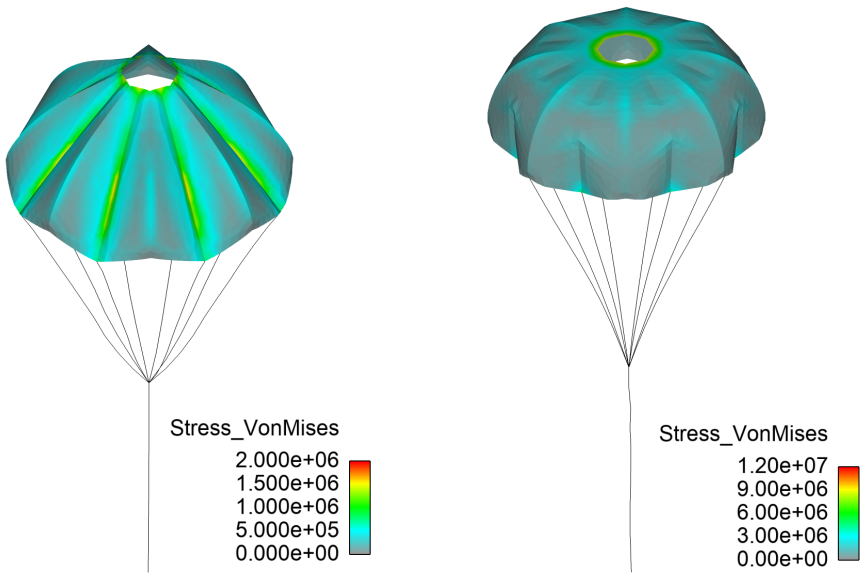

Figure 9 – Von misses stress in canopies at steady state phase (Left $v_\infty = 3\ m/s$ and right $v_\infty = 14\ m/s$

Maximum stress occurs when snatch shock is happening. As can be seen in Figure 10. For $v_\infty = 3$

m/s maximum stress is located on the vent edge. This is caused by high flow thru the vent. For $v_\infty = 14\ m/s$ maximum stress is located at the connections of lines and canopy. There is also second critical area in the center of gore edges.

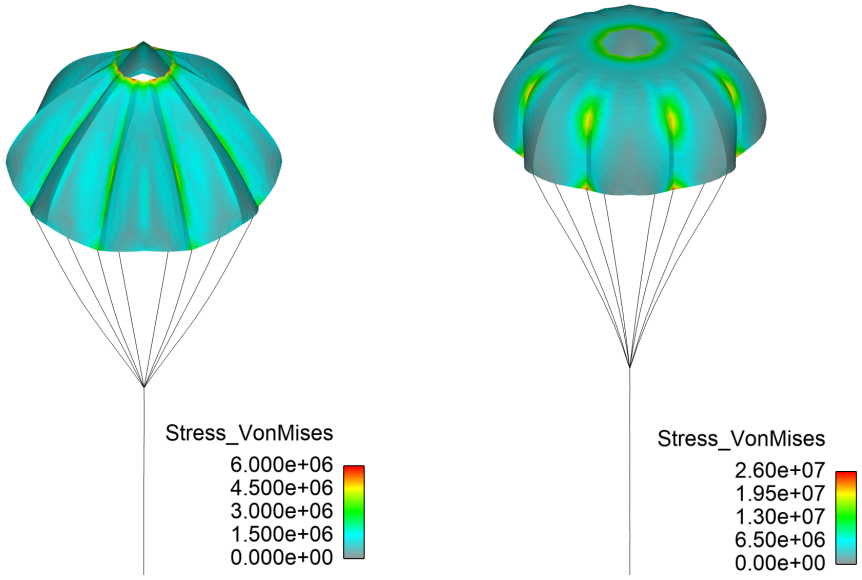

Figure 10 – Von misses stress in canopies at Snatch force moment (Left $v_\infty = 3\ m/s$ and right $v_\infty = 14\ m/s$

4.2 Flow field analysis

The visualization of the fluid flow for the 3 m/s, 8 m/s and 14 m/s cases can be seen in Figure 11, where is velocity field, and in Figure 12, where is relative pressure field.

In Figure 12 it can be seen for all free-stream velocities that a vortex ring is formed behind the parachute, which is typical for parachutes. For a free-stream velocity of 3 m/s there is only one vortex ring, for a speed of 8 m/s there is 1 vortex rings and for a speed of 14 m/s there is one vortex ring and a series of small vertices that break off at the canopy skirt. The detachment of the smaller vertices is unstable and therefore no symmetry is seen. The positions of the vortex rings are different at $t = 1s$, this is due to the different free-stream velocities and the fact that this is a transient simulation and not a steady state simulation.

In Figure 11, it can be seen that the shape of the canopy for the 3 m/s velocity is significantly different from the others. The velocity of air flowing through the vent is approximately 1.5 times the free airflow, whereas for the other velocities. Due to the larger amount of outgoing air, the canopy is not fully filled with air. With different canopy shape, the canopy achieves higher drag coefficients, as can be seen in Figure 5.

For a more accurate comparison of steady-state flow, the simulation would need to be run over a longer time period, for lower velocities, to allow the flow to permeate the entire domain. This is associated with higher computational time.

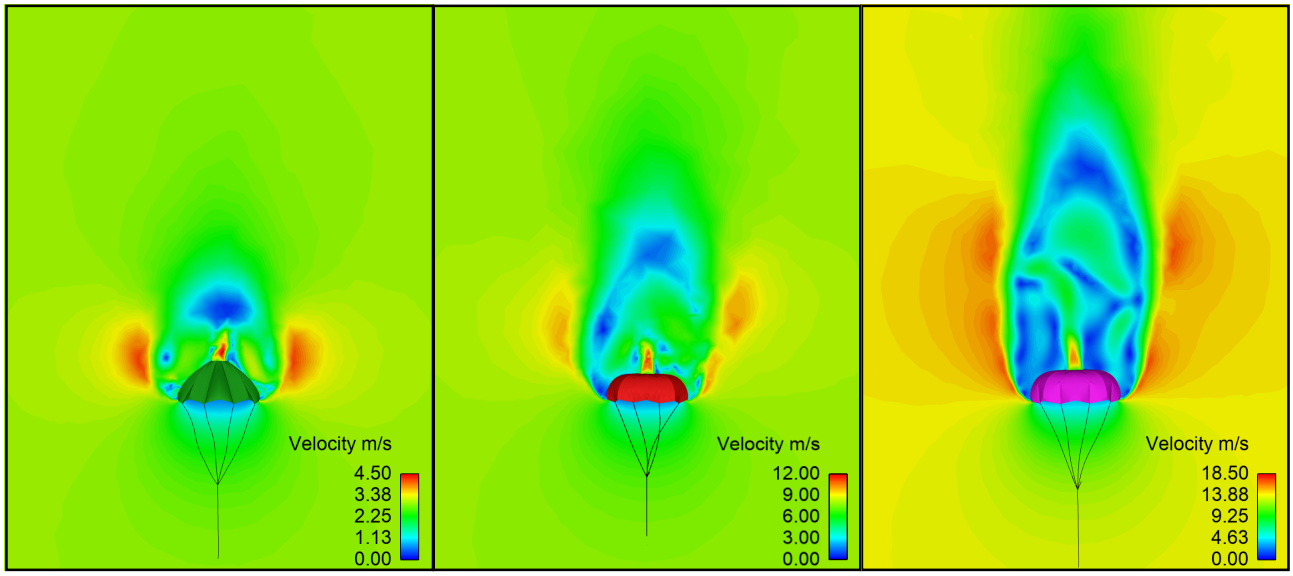

Figure 11 – Velocity flow field for 3, 8, 14 m/s at $t = 1s$

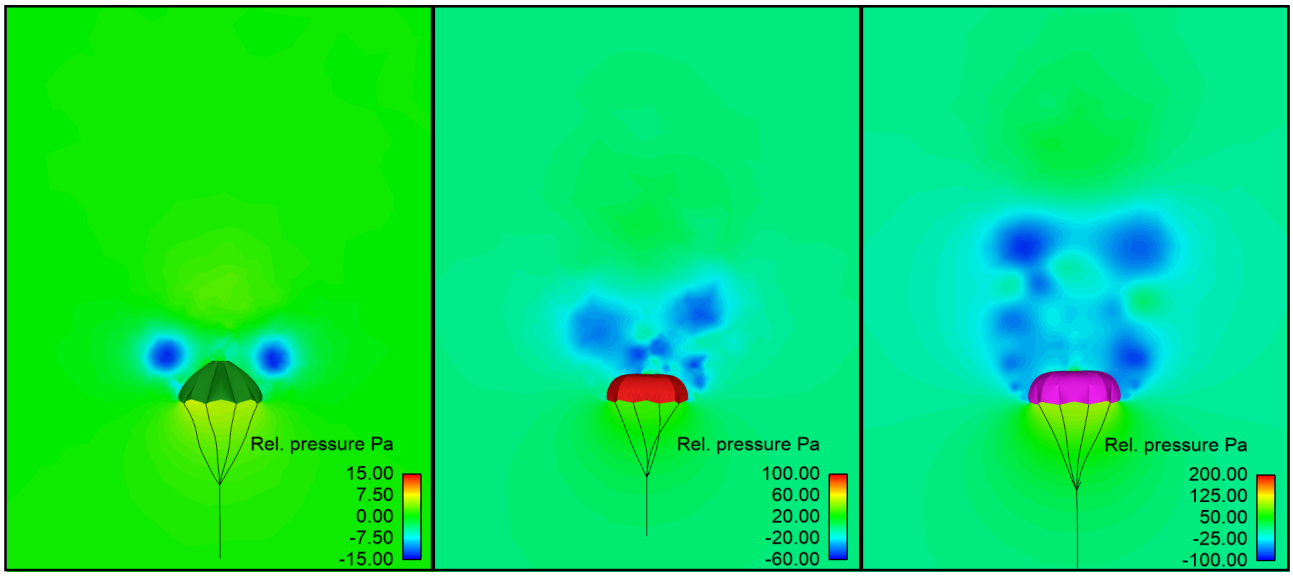

Figure 12 – Pressure field for 3, 8, 14 m/s at $t = 1s$

5. Conclusion

In conclusion, a workflow for analyzing infinite mass inflation of parachutes has been successfully developed, with results that align well with predicted behavior. The steady-state parachute shapes observed in the simulations closely matched experimental measurements, confirming the validity of the results. The parachute under analysis demonstrated a drag coefficient of $c_D = 0.75$. Additionally, the shape of the inflated canopy was found to be highly dependent on the opening velocity, revealing significant differences in behavior due to variations in the flow of bypassed air.

This methodology offers a foundational approach for exploring the feasibility of controlling parachute canopy inflation, potentially expanding the range of applications for parachute systems. Future work will involve applying this workflow to analyze the effects of sliders, with the resulting simulations integrated into a system model for a passive aircraft rescue system. This will contribute to improving parachute design and functionality in real-world application.

6. Contact Author Email Address

xkaspa43@vutbr.cz

7. Copyright Statement

8. Acknowledgement

This work has been supported by the project No. FSI-S-23-8163 funded by The Ministry of Education, Youth and Sport (MEYS, MŠMT in Czech) institutional support.

References

[1] Larsen E. Jirase A. Rose T. Noetscher Bergeron K., Ghoreyshi H. Near-body/cartesian off-body simulations for c-17 and extraction parachute. In *AIAA AVIATION Forum*, 2020.

[2] Lawson M.R. Borrvall T. On accuracy and stability of implicit time integration schemes for rotating structures. In *Proceedings of the 16th International LS-DYNA® Users Conference*, 2020.

[3] Pastor P. Perin B. Chambe J. E., Miguel C. Methodology for icfd calculation with a light deformable structure–application to ram-air parachute. In *AIAA SciTech Forum and Exposition, 2024*, 2024.

[4] Charles R. D. Simulation of the baseline performance characteristics of a ram-air parachute. In *24th AIAA Aerodynamic Decelerator Systems Technology Conference*, 2017.

[5] McLaughlin T. Noetscher G. Rose T. Fagley C., Seidel J. Computational study of air drop control mechanisms for cruciform parachutes. In *24th AIAA Aerodynamic Decelerator Systems Technology Conference, 2017*, 2017.

[6] Tang Q. Gao X., Zhang Q. Fluid-structure interaction analysis of parachute finite mass inflation. 2016.

[7] Schwing Greathouse J. S. Study of geometric porosity on static stability and drag using computational fluid dynamics for rigid parachute shapes. In *23rd AIAA Aerodynamic Decelerator Systems Technology Conference*, 2015.

[8] T. W. Knacke. *Parachute recovery systems*. Para, Santa Barbara, 1992.

[9] Lapoujade V. Le Garrec M., Poncet A. Parachute deployment simulations using ls-dyna icfd solver and strong fsi coupling. In *12th European LS-DYNA Conference 2019*, 2019.

[10] NTSB. *Review of US Civil Aviation Accidents Calendar Year 2011*. National Transportation Safety Board, 2011.

[11] KY P. *EASA Anual Safety Review 2018*. EASA, 2018.

[12] Bordenave P. Larrieu C. Simond C. Perin B., Belloc H. Fluid-structure interaction simulation of ram air parachutes - an application for a kite -. In *23rd AIAA Aerodynamic Decelerator Systems Technology Conference*, 2015.

[13] Patoux A. Perin B. Modeling method of ram-air parachute with ansys-dyna®. In *26th AIAA Aerodynamic Decelerator Systems Technology Conference*, 2022.

[14] Kavanaugh J. Potvin J. A second look at geometric porosity, as revealed by computational fluid dynamics (cfd). In *AIAA Aerodynamic Decelerator Systems (ADS) Conferences*, 2013.

[15] Charles R.D. Optimizing extraction parachute operational parameters. In *23rd AIAA Aerodynamic Decelerator Systems Technology Conference*, 2015.

[16] Bergeron K. Rose T., Noetscher G. Simulation and testing assessment of cruciform parachute using ls-dyna ale. In *15th International LS-DYNA Conference 2018*, 2018.

[17] Sathe S. Tezduyar T. E. Modelling of fluid-structure interactions with the space-time finite elements: Solution techniques. *International Journal for Numerical Methods in Fluids*, 2007.

[18] Berland J. C. Gargano B. Tutt B., Taylor A. The use of ls-dyna to assess the performance of airborne systems north america candidate atps main parachutes. In *18th AIAA Aerodynamic Decelerator Systems Technology Conference and Seminar*, 2005.

[19] Noetscher G. Tutt B., Roland S. Charles R. D. Finite mass simulation techniques in ls-dyna®. In *21st AIAA Aerodynamic Decelerator Systems Technology Conference and Seminar 2011*, 2011.

[20] Taylor A. Tutt B. The use of ls-dyna to simulate the inflation of a parachute canopy. In *18th AIAA Aerodynamic Decelerator Systems Technology Conference and Seminar*, 2005.

[21] Guillaume C. Christine E. Yves C., Pascal B. Improvements in fluid structure interaction simulations of parachutes using ls-dyna®. In *21st AIAA Aerodynamic Decelerator Systems Technology Conference and Seminar*, 2011.